

# Factors affecting prior austenite grain size in low alloy steel

S. Maropoulos · S. Karagiannis · N. Ridley

Received: 21 November 2005 / Accepted: 30 January 2006 / Published online: 30 November 2006  
© Springer Science+Business Media, LLC 2006

**Abstract** The effect of varying normalising and hardening temperatures on the prior austenite grain size in a low alloy Cr–Mo–Ni–V steel has been examined. An initial relative insensitivity of grain size to increasing austenitising temperature was observed followed by a sudden growth of grains at approximately 1000 °C. A detailed study of the precipitates in the steel showed the presence of a bimodal size distribution of vanadium carbides. The grain size increase is attributed to a decrease in volume fraction and an increase in size of  $V_4C_3$  particles with increasing temperature.

## Introduction

High strength low alloy (HSLA) steels containing alloying elements are widely used in construction, pipeline and general engineering applications. The role of microalloying is to improve both the strength and toughness of steels by grain refinement. Grain refinement results from the inhibition of austenite grain growth during reheating and retardation of recrystallization by the fine carbide and nitride precipitates

[1–4]. Vanadium is known to be very effective in achieving grain refinement through the formation of  $V_4C_3$  and VN particles. It tends to partition to interdendritic regions during solidification along with carbon and nitrogen [5, 6], which can lead to inhomogeneous precipitation of C,N-rich particles on solidification [7], particularly at grain boundaries, [8].

Grain coarsening in carbon steels involves gradual growth of grains as the temperature is increased [9]. However, in steels with additions of grain refining elements such as aluminium, niobium, vanadium and titanium, all of which produce small sparingly soluble precipitates, a sudden abnormal growth of grains has been reported [10–12]. The work reported here is a detailed metallographic study aimed at understanding the mechanism by which such a growth of prior austenite grains occurs and identifying the role played by vanadium carbide particles in a heat treated medium carbon low alloy steel.

## Experimental procedures

### Material composition and heat treatment

Sections from a large cylindrical forging (9 m long, 280 mm diameter) were supplied. The material had been given a cyclic anneal, aimed at removing hydrogen, involving holding at various temperatures between 280 and 900 °C for different times followed by furnace cooling to 400 °C and then air cooling to room temperature. The steel was a high quality electroslag remelted steel of the composition given in Table 1. Heat treatment was carried out on annealed material to determine the effect of two-cycle austenitising, prior

---

S. Maropoulos (✉) · S. Karagiannis  
Department of Mechanical Engineering, University of Applied Science of West Macedonia, Pl. 25 Martiou 5, Kóila, 50100 Kozani, Greece  
e-mail: maropou@otenet.gr

N. Ridley  
Materials Science Centre, University of Manchester, Grosvenor Street, Manchester M1 7HS, UK

**Table 1** Chemical analysis by Quantivac, wt. %

C	Ni	Cr	Mo	V	Cu	Mn	Si	P	S
0.38	3.37	0.9	0.73	0.2	0.2	0.45	0.22	0.005	0.002

to quenching and tempering, on the microstructure. The initial austenitising was followed by air cooling and will subsequently be referred to as normalising. The second austenitising treatment involved oil quenching and will be referred to as hardening.

The austenitising temperatures for normalising and hardening were varied from 930 to 850 °C and 910 to 830 °C, respectively. Tempering was carried out at a fixed temperature of 620 °C and it was followed by oil quenching to room temperature. The austenitising times for the normalising and hardening treatments were 4 and 3 h respectively, while the tempering time was 6 h. The exact heat treatment schedule is given in Table 2. The heat treatments were carried out in a muffle furnace using blocks of steel measuring 120 × 60 × 11 mm painted with a clay solution to prevent oxidation.

#### Optical metallography

Specimens for optical metallography were ground and mechanically polished to 1 µm finish. Etching was done using either 2% nital or a mixture composed of 70% of 2% nital and 30% of saturated aqueous picric acid for 10–20 s.

**Table 2** Heat treatment schedule and prior austenite grain size

Code	Normalising temperature (°C)	Hardening temperature (°C)	Austenite grain size after normalizing (µm)	Austenite grain size after hardening (µm)
1	–	910	–	8.2
2	–	890	–	7.6
3	–	870	–	5.5
4	–	850	–	4.6
5	–	830	–	4.0
6	930	910	11.2	7.1
7	930	890	11.2	6.1
8	930	870	11.2	5.6
9	930	850	11.2	5.4
10	930	830	11.2	5.3
11	910	890	10.0	5.6
12	910	870	10.0	4.9
13	910	850	10.0	4.6
14	910	830	10.0	4.0
15	890	870	10.0	5.7
16	890	850	10.0	4.9
17	890	830	10.0	3.9
18	870	850	8.1	5.0
19	870	830	8.1	4.4
20	850	830	6.4	4.1

Revealing the prior austenite grain boundaries of martensitic steels is always a problem and several etching methods are reported in the literature [13–15]. All these methods are rather time consuming and do not guarantee the results. A preferential oxidation method, recommended in British Standard 4490 was employed. For this, 1 cm<sup>3</sup> cubes of material were polished to 1 µm finish and etched in 2% nital. They were then heat treated as in Table 2 in a dry argon atmosphere. Five minutes before quenching from the austenitising temperature the argon was turned off and air was let in the furnace. After quenching the specimens, which showed only marginal oxidation on the pre-polished surfaces, were re-polished on a 1 µm diamond wheel and etched in 2% nital. Austenite grain sizes were determined by the mean linear intercept method using at least 500 intercepts.

#### Electron microscopy and X-ray diffraction

Transmission electron microscopy involved the examination of thin foils and extraction replicas. The carbide distributions in the steels were examined using carbon replicas. For surface replicas, used for carbide microanalysis, the samples were etched in 0.5% nital while for extraction replicas, used for carbide size measurements, the samples were deeply etched in 2% nital. About 20 particles from each of the different carbide morphologies present in the steels were analyzed using the energy dispersive X-ray detector fitted on a Philips 400T electron microscope. Diffraction patterns were also taken from some of the carbides

analysed. In addition, the carbides present were extracted electrolytically and the residues were examined with X-ray diffraction using copper  $K\alpha$  radiation.

To determine the size of the vanadium carbides in the microstructures several photographs were taken from extraction replicas. At least 500 particles were counted and the mean particle diameter,  $x_s$ , and the standard deviation,  $\sigma_s$ , of the raw data were used to calculate the mean particle diameter,  $x_v$ , and the standard deviation,  $\sigma_v$ , of the volume distribution [16]. For fractographic studies, specimens were examined with a Philips SEM 505 electron microscope fitted with an X-ray detector. Quasicleavage facet size, known to be equivalent to the martensite packet size, was obtained by averaging the dimensions of at least 150 facets on Charpy specimens fractured at  $-196^\circ\text{C}$ , measured directly from the screen of the SEM.

## Results

### The microstructures

The microstructures, involved in the various stages of the heat treatment employed, were examined in a previous study by the authors [17]. The microstructures were martensitic, even in the as-normalised condition, with the martensite laths exhibiting a high dislocation density and a large number of auto-tempered carbides. The lath morphology was retained after tempering at  $620^\circ\text{C}$ . The apparent lath width was similar in all stages of heat treatment at about  $0.3\ \mu\text{m}$ . A high dislocation density was observed in all structures with the dislocations arranged as sub-cells in the tempered condition.

The microstructure of a specimen quenched from  $1065^\circ\text{C}$ , prepared so as to reveal the prior austenite grains and then deeply etched in 70% nital-30% picric acid, is shown in Fig. 1. The typical structure of lath martensite can be seen with a number of packets of parallel laths within the large austenite grains.

### Carbide distribution

Examination of carbon extraction replicas showed the presence of four distinct carbide morphologies in the tempered and in the as-received microstructures [17]. Lath boundaries were outlined with long, fairly continuous carbide films. Three types of precipitates were seen within the laths; (1) globular carbides, often associated with sub-grains, of diameter 30–100 nm, (2) spherical precipitates of very small size ( $<25\ \text{nm}$ ) and (3) thin, rod-shaped carbides lying parallel or at  $45^\circ$  to

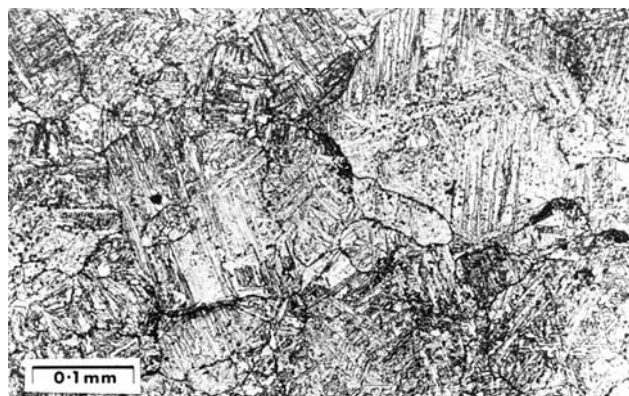


**Fig. 1** The microstructure of material as quenched from  $1065^\circ\text{C}$  prepared so as to reveal the prior austenite grains

the longitudinal axis of the laths. On prior austenite grain boundaries globular carbides were sometimes seen.

Electron diffraction on several particles and X-ray diffraction on extracted carbide residues showed that the majority of the carbides were cementite with fairly large amounts of chromium, molybdenum, manganese and vanadium in solution, so that the carbides may be better described as  $\text{M}_3\text{C}$ . The X-ray diffraction results indicated that a small amount of  $\text{V}_4\text{C}_3$  was also present in tempered and in as-received material. Examination of extraction replicas showed that as-received material contained a number of fairly large globular vanadium carbide particles whereas the tempered specimens contained much finer vanadium carbides.

The vanadium carbides were further studied using as-normalised and as-quenched specimens. Figure 2a, b show the distribution of precipitates in specimens normalised from  $890^\circ\text{C}$  and quenched from  $830^\circ\text{C}$ , respectively. Electron diffraction and X-ray diffraction on extracted carbide residues of as-normalised and as-quenched specimens showed that only  $\text{V}_4\text{C}_3$  carbides were present. It is quite possible, however, that other types of carbide were present but in amounts below the detection limit of the diffractometer used ( $\sim 2\%$ ).

Using the solubility product of Woodhead [18], for a bulk composition of 0.38% carbon and 0.2% vanadium, the solution temperature of  $\text{V}_4\text{C}_3$  was found to be  $1019^\circ\text{C}$ . The amount of vanadium dissolved at the different austenitising temperatures and the volume fraction of undissolved vanadium carbide was determined, Table 3.

The volume fraction of cementite, 5.8%, was assumed to be the same for all heat treatment conditions. It was calculated from stoichiometry assuming all the carbon was out of solution after tempering at  $620^\circ\text{C}$  and in the form of  $\text{Fe}_3\text{C}$ .

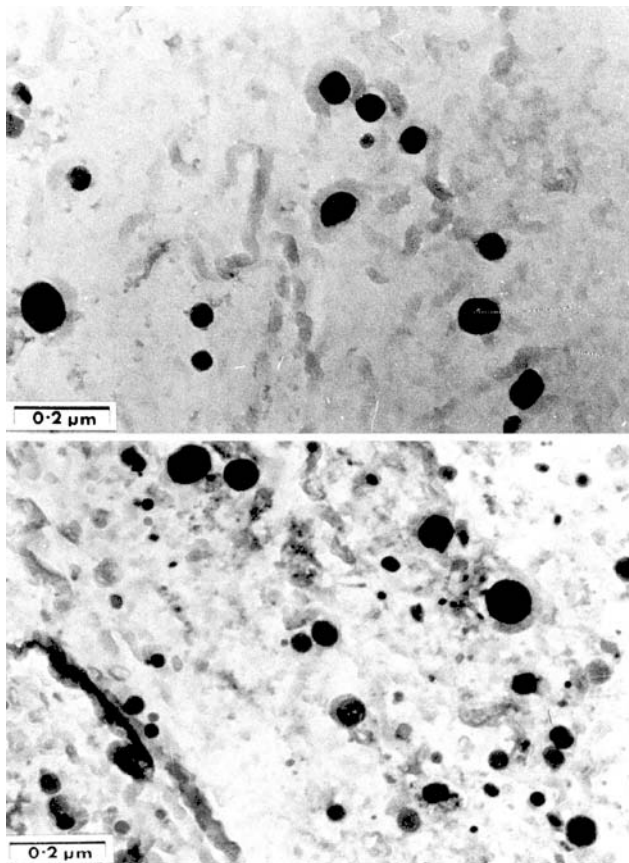


**Fig. 2** Vanadium carbides in material (a) as-normalised from 890 °C and (b) normalised from 890 °C and quenched from 830 °C

#### Prior austenite grain size

The prior austenite grain sizes (mean linear intercepts) for all the heat treatment conditions tested and the standard deviations of the measurements are given in Table 2. The austenite grain sizes after the initial austenitising are also included in Table 2. As can be seen the grain size after the second austenitising was always smaller than that after the initial austenitising, irrespective of the austenitising temperatures employed. The variation in austenite grain size with hardening temperature (second austenitising), for the normalising temperatures of 930 (first austenitising), is shown in Fig. 3. As can be seen there was a small increase in grain size with increasing hardening temperature. However, the grain size remained very small, below  $\sim 7 \mu\text{m}$ , throughout the hardening temperature range used, Fig. 4. A similar increase in austenite grain size with increasing hardening temperature was observed for un-normalised material.

In an attempt to explain the fine grain sizes observed, the variation in grain size with austenitising

**Table 3** Amount of vanadium dissolved during austenitising and content of remaining undissolved after each austenitising treatment

Code	Hardening temperature (°C)	Vanadium in solution wt. %	V <sub>4</sub> C <sub>3</sub> vol. % after first austenitising (primary)	V <sub>4</sub> C <sub>3</sub> vol. % after second austenitising (secondary)
Non-normalised				
1	910	0.062	0.248	–
2	890	0.048	0.272	–
3	870	0.037	0.291	–
4	850	0.028	0.307	–
5	830	0.021	0.321	–
$T_{\gamma}^N = 930^{\circ}\text{C}$				
...	AN	0.079	0.218	–
6	910	0.062	0.218	0.031
7	890	0.048	0.218	0.054
8	870	0.037	0.218	0.076
9	850	0.028	0.218	0.090
10	830	0.021	0.218	0.102
$T_{\gamma}^N = 910^{\circ}\text{C}$				
...	AN	0.062	0.248	–
11	890	0.048	0.248	0.024
12	870	0.037	0.248	0.044
13	850	0.028	0.248	0.059
14	830	0.021	0.248	0.073
$T_{\gamma}^N = 890^{\circ}\text{C}$				
...	AN	0.048	0.272	–
15	870	0.037	0.272	0.018
16	850	0.028	0.272	0.035
17	830	0.021	0.272	0.047
$T_{\gamma}^N = 870^{\circ}\text{C}$				
...	AN	0.037	0.291	–
18	850	0.028	0.291	0.014
19	830	0.021	0.291	0.027
$T_{\gamma}^N = 850^{\circ}\text{C}$				
...	AN	0.028	0.307	–
20	830	0.021	0.307	0.011

$T_{\gamma}^N$  austenitising temperature for normalizing; AN as normalized

temperature was studied over the temperature range 830–1070 °C. The grain coarsening curve for as-received material held for 4 h at various temperatures is shown in Fig. 5. After a small initial increase at low temperatures, Fig. 6a,b, the grain size remained almost constant at about 10  $\mu\text{m}$  and then at some critical temperature,  $\sim 1000^{\circ}\text{C}$ , very large austenite grains developed (up to 200  $\mu\text{m}$ ) resulting in a mixture of coarse and fine grains, Fig. 6c,d. With increasing temperature more of these grains developed and eventually the majority of the grains became coarse.

The variation in prior austenite grain size with normalising temperature for the hardening temperature of 830 °C is shown in Fig. 7. As can be seen there was a very small increase in grain size as the normalising temperature increased. Similar behaviour was

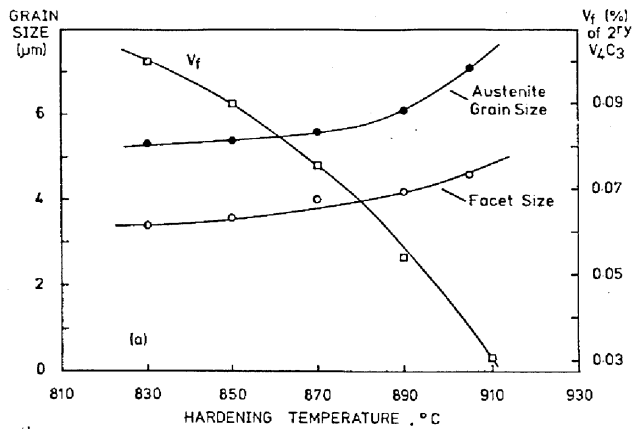


**Fig. 3** The variation in prior austenite grain size, facet size and volume fraction of secondary V<sub>4</sub>C<sub>3</sub> with hardening temperature for material normalised from 930 °C

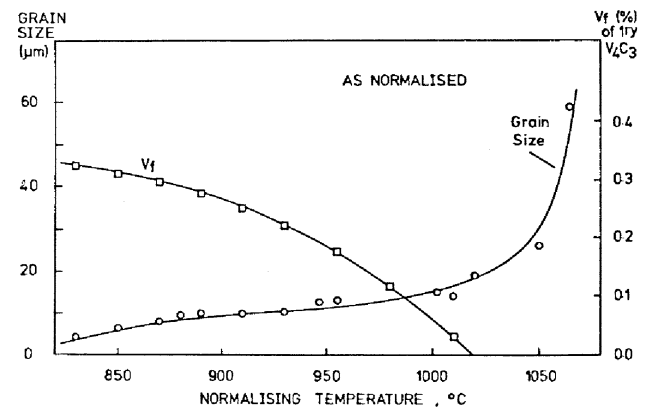


**Fig. 5** The grain coarsening curve for as-normalised material and the volume fraction of primary V<sub>4</sub>C<sub>3</sub>

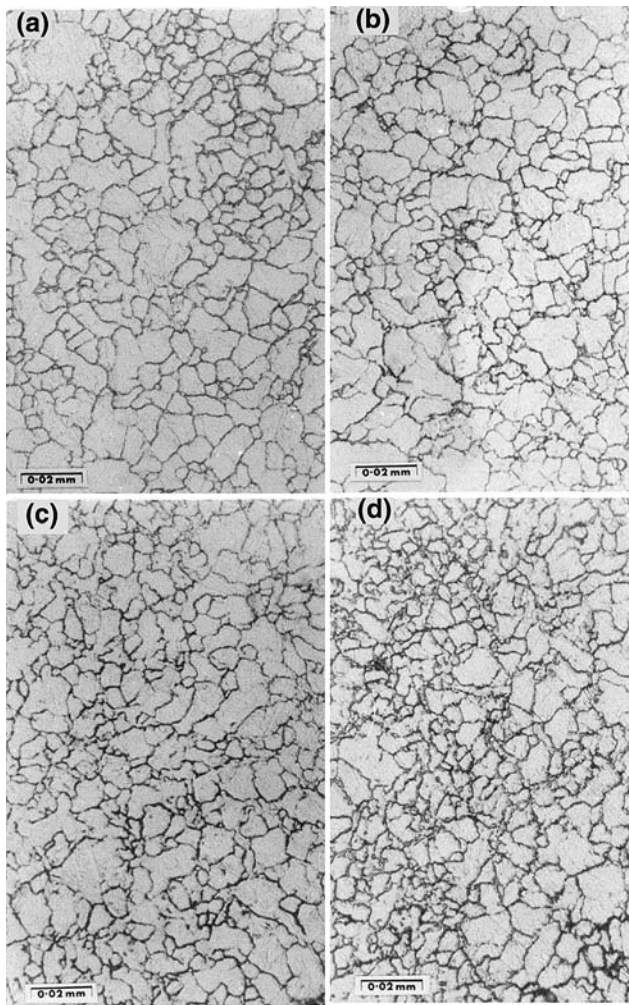


**Fig. 4** The prior austenite grain structures of material normalised from 930 °C and hardened from (a) 910 °C, (b) 890 °C, (c) 850 °C and (d) 830 °C

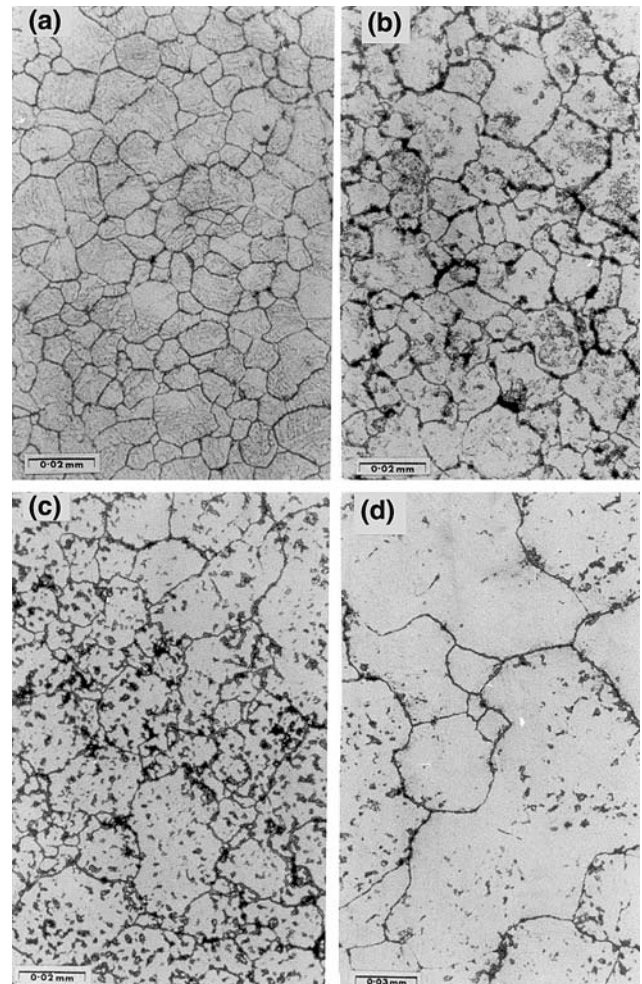


**Fig. 6** The prior austenite grain structures of material as-normalised from (a) 870 °C, (b) 955 °C, (c) 1010 °C and (d) 1065 °C

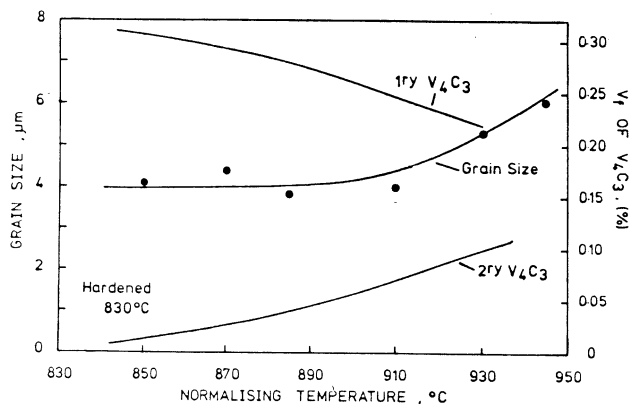


**Fig. 7** The variation in prior austenite grain size with normalising temperature for material hardened from 830 °C and the volume fraction of primary and secondary  $V_4C_3$

observed for the hardening temperature of 850 °C, Table 2.

## Discussion

### Effect of heat treatment on the distribution of vanadium carbides

The vanadium carbides were investigated in a previous study by the authors [19]. It was shown that after the cyclic annealing treatment most of the vanadium is out of solution in the form of coarse particles. It is not clear at which stage of the cyclic annealing treatment these coarse particles were formed but it is thought that they were developed during holding at 900 °C for 10 h. Vanadium carbides are known to coarsen at a very rapid rate by a mechanism of dislocation coarsening controlled by pipe diffusion [20]. Ballinger and Honeycombe [20] found that high dislocation densities resulted in increased particle coarsening rates. Before annealing the material would be expected to have a mixed structure of martensite and bainite, formed during cooling from the forging temperature, and thus, a high dislocation density, which may account for the coarse vanadium carbides observed.

When annealed material is heated to the first austenitising temperature the coarse vanadium carbide particles will start dissolving until the equilibrium volume fraction of undissolved  $V_4C_3$  for the particular austenitising temperature is reached, Table 3. Thus, an as-normalised specimen is expected to contain carbide particles (primary  $V_4C_3$ ) finer than those of the annealed material, and a few large particles that remained undissolved, plus a certain amount of

vanadium in solution in austenite,  $V_\gamma$ . When the as-normalised structure is heated to the second (lower) austenitising temperature some of the vanadium that had gone into solution during the first austenitising will precipitate as very fine  $V_4C_3$  (secondary  $V_4C_3$ ) until the equilibrium  $V_\gamma'$  for the second austenitising temperature is reached, Table 3. Thus, a specimen as-quenched from the second austenitising temperature will contain primary  $V_4C_3$ , secondary  $V_4C_3$ , and some vanadium in solution in austenite,  $V_\gamma'$ .

The primary vanadium carbide particles are thought to remain unaltered during the second austenitising treatment. Some particle coarsening is likely to take place but this may be balanced by the particle dissolution, which will also occur. A similar observation was reported by Webster and Allen [21], also working with vanadium carbides, and by Gladman and Dulieu [22] for aluminium nitride particles. The secondary vanadium carbides are thought to be nucleated at the  $\gamma/\alpha$  interface as very fine precipitates [20, 23] during heating to the austenitising temperature. Most of these dissolve rapidly during holding at the austenitising temperature, but the rest agglomerate and produce fewer and larger, but still fine, stable carbides [21].

The size of primary vanadium carbides was measured from extraction replica micrographs of specimens as-normalised from the temperature range 850–955 °C. The results are given in Table 4. The parameter  $M$  reported is given by

$$M = (x_v^2 + \sigma_v^2)^{1/2} \quad (1)$$

where  $x_v$  is the mean carbide diameter of the volume distribution and  $\sigma_v$  the standard deviation, and is considered as a better description of the particle size when a distribution of particle sizes is involved [24]. This parameter will be used in the calculations of Section ‘Predicted versus observed grain size’.

**Table 4** The size of primary vanadium carbides (nm) in material as-normalised at various temperatures

Normalising temperature (°C)	$x_s$ (nm)	$\sigma_s$ (nm)	$x_v$ (nm)	$\sigma_v$ (nm)	$M$ 1 <sup>st</sup> (nm)
955	26	16	19	10	22
945	42	19	35	16	38
930	47	23	38	19	42
890	46	20	39	17	43
850	49	24	40	19	45

$x_s$  = mean particle diameter and  $\sigma_s$  = standard deviation as measured from extraction replicas

$x_v$  = mean carbide diameter and  $\sigma_v$  = standard deviation of the volume distribution,  $M = (x_v^2 + \sigma_v^2)^{1/2}$

**Table 5** The size of vanadium carbides (nm) in as-quenched material for the normalising temperature of 930°C (primary and secondary V<sub>4</sub>C<sub>3</sub> particles)

Code	Hardening temperature (°C)	$x_s$ (nm)	$\sigma_s$ (nm)	$x_v$ (nm)	$\sigma_v$ (nm)	$M$ (1ry+2ry) (nm)
6	910	45	20	37	17	41
7	890	31	18	24	13	27
8	870	21	13	15	10	18
9	850	18	8	15	7	16
10	830	20	12	15	9	17

As can be seen from Table 4 the size of the primary carbides decreases as the normalising temperature is increased and this confirms the suggestion that the primary carbides arise from the dissolution of coarse V<sub>4</sub>C<sub>3</sub> particles.

The size of the vanadium carbides in as-quenched specimens was measured for some of the heat treatment conditions tested, Table 5. The value of  $M(1ry + 2ry)$  includes contributions from both types of carbide, primary and secondary. As can be seen, for the normalising temperature of 930 °C,  $M(1ry + 2ry)$  decreases with decreasing hardening temperature. Assuming that the size of the primary carbides remained constant at  $M(1ry) = 42$  nm the decrease in  $M(1ry + 2ry)$  can be explained by the calculations shown in Table 3. The volume fraction of secondary V<sub>4</sub>C<sub>3</sub> increases with decreasing hardening temperature and, therefore, at low temperatures, there will be a larger number of fine secondary particles which results in a lower  $M(1ry + 2ry)$ . This is demonstrated in Fig. 8. The increase in  $M(1ry + 2ry)$  as the normalising temperature is decreased for the constant hardening temperature of 830 °C, Table 6, is a result of the observed increase in the size of the primary carbides and the decrease in volume fraction of secondary V<sub>4</sub>C<sub>3</sub> at lower normalising temperatures.

Effect of temperature on prior austenite grain size

The observed increase in prior austenite grain size with increasing austenitising temperature, Figs. 5 and 6, is typical of the grain growth commonly observed in steels with grain refining additions. This type of grain growth is sometimes referred to as secondary recrystallisation and occurs in steels containing elements such as aluminium, niobium, vanadium and titanium, all of which produce fine precipitates. It is different from the other type of grain coarsening observed in carbon steels where gradual growth of grains takes place as the temperature is increased, rather than the

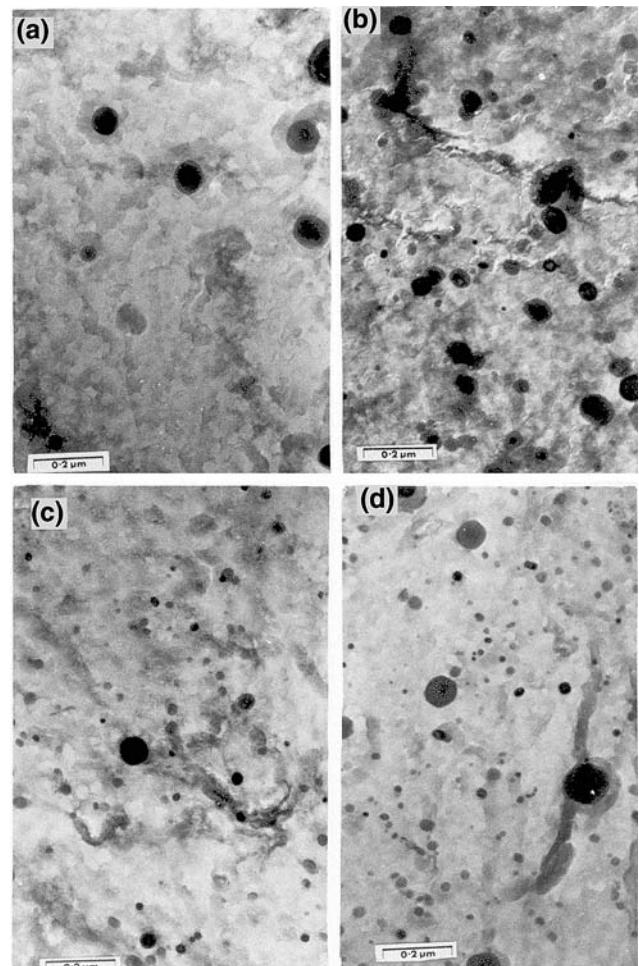


**Fig. 8** The volume fraction of secondary V<sub>4</sub>C<sub>3</sub> increases with decreasing hardening temperature (a) 910 °C, (b) 890 °C, (c) 850 °C and (d) 830 °C

sudden abnormal growth of only a few grains observed in the present work.

The initial relative insensitivity of grain size to increasing temperature, Fig. 5, is thought of as an incubation period after which some of the crystals start to grow at the expense of their neighbours. The causes of nucleation are not entirely clear [25] but grain coalescence could well produce this effect. It is relatively easy to understand the growth that occurs

**Table 6** The size of vanadium carbides (nm) in material hardened from 830°C (primary and secondary V<sub>4</sub>C<sub>3</sub> particles)

Code	Normalising temperature (°C)	$x_s$ (nm)	$\sigma_s$ (nm)	$x_v$ (nm)	$\sigma_v$ (nm)	$M$ (1ry + 2ry) (nm)
....	945	15	9	10	7	12
10	930	20	12	15	9	17
17	890	30	16	23	13	26
20	850	33	15	27	13	30

once it starts for the following two reasons. Firstly, the enlarged crystals soon become grains with a large number of sides as they consume their smaller neighbours, Fig. 6(d). Grains with many sides possess boundaries, which are concave away from their centres and, according to early suggestions [26] should become larger.

Harker and Parker [26] proposed that the boundary atoms in the crystal on the concave side of the boundary are more tightly bound than the boundary atoms in the crystal on the convex side, because they are more closely surrounded by neighbouring atoms of the same crystal. This tighter binding of the atoms on the concave side of the boundary should make the rate at which atoms jump across the boundary from the convex to the concave crystal greater than in the opposite direction. The greater the curvature of the boundary then, the greater should this effect be and the faster the movement of the crystal boundary [25].

The alternative reason why the enlarged crystals should grow comes from Hillert [27] who considered the relationship between the rate of growth of metal grains, and the energy changes involved. It was recognised that large grains grow at the expense of small ones, and a simple model of the energy change,  $E$ , was developed, in which:

$$-E = K(1/Rc - 1/R) \quad (2)$$

where  $R$  is the radius of any grain,  $Rc$  is a critical radius and  $K$  is a constant. This model indicates that the growth of grains larger than the critical size would cause a decrease in energy, whereas the growth of grains smaller than the critical size would cause an increase in energy. This would prevent the growth of the smaller grains [28]. To summarise, secondary recrystallisation is a case of exaggerated grain growth occurring as a result of surface energy considerations.

The volume fraction of  $V_4C_3$  present at the austenitising temperatures is plotted in Fig. 5. As can be seen there is excellent agreement between the solution temperature of vanadium carbide (1019 °C) and the temperature at which abnormal grain growth begins (~1010 °C). Erasmus [29] studied the effect of vanadium on the austenite grain coarsening temperature of 0.2% carbon steel and found that the grain coarsening temperature was closely related to the solution temperature of vanadium nitride. Gladman and Pickering [28] however, found that grain coarsening in their aluminium and niobium steels occurred well below the solution temperature of aluminium nitride and niobium carbonitride, respectively. They attributed these

observations to an overlarge particle size effect, whereby the precipitated AlN and Nb(CN) particles become too large to retard grain growth effectively.

It is evident from Fig. 5 that vanadium carbide particles played an important role in controlling the austenite grain size. Second phase particles, such as carbides and nitrides, can influence grain growth because they decrease the grain boundary area and hence the overall boundary energy [28]. A number of attempts have been made to develop a satisfactory theory for the effects of second phase particles on grain growth and grain size. Zener [30] considered the equilibrium between the driving force per unit area for grain boundary movement and the restraining force due to second phase particles sitting on the grain boundary. Zener developed the following relationship,

$$R_{\max} = 4r/3f \quad (3)$$

where  $R_{\max}$  is the maximum radius of curvature of the grain and  $r$ ,  $f$  the particle radius and volume fraction, respectively. This relationship assumes spherical particles and a uniform distribution of particles, neither of which can be realised in a real metal. However, it gives a good approximation of the effect of precipitates on grain growth [25]. Since it can be assumed that the radius of curvature is directly proportional to the grain size [25], the above equation shows that the ultimate grain size to be expected, in the presence of second phase particles, is dependent on the particle size and volume fraction.

#### Predicted versus observed grain size

Gladman and Pickering [28] suggested that Eq. 3 indicates a much larger equilibrium grain size than is observed because the Zener model overestimates the driving force for grain growth. However, experimental observations [31, 32] have shown that the Zener equation is essentially correct. The Zener equation was used to predict the maximum equilibrium grain size for the heat treatment conditions for which vanadium carbide data, size and volume fraction, is available and for specimens in the as normalised condition. As can be seen from Fig. 9a the predicted grain sizes follow the same trend of increasing size with increasing normalising temperature. However, the predicted values are significantly higher than the observed grain sizes. Similarly, for the increase in grain size with hardening temperature after normalising from 930 °C, Fig. 9b the predicted values follow the same trend but are much higher than the observed



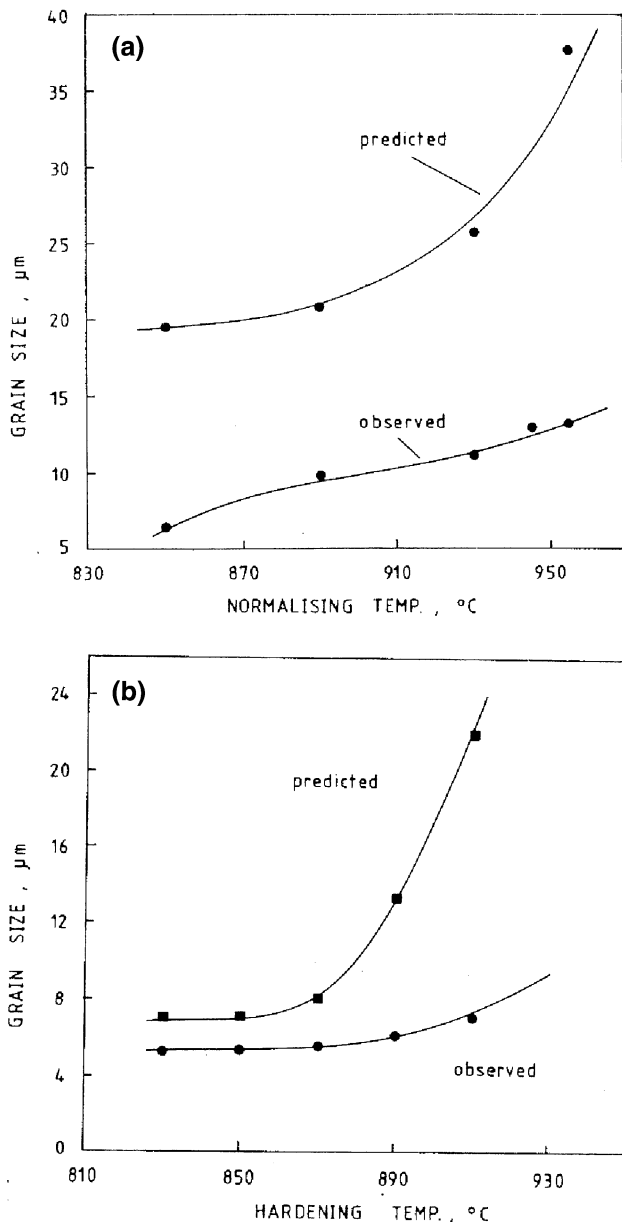


**Fig. 9** The variation in predicted and observed prior austenite grain size with (a) normalising temperature in as-normalised material and (b) hardening temperature in material normalized from 930 °C

ones. Although there is a large discrepancy between observed and predicted values, the variation in grain size in as-normalised specimens and in specimens hardened from different temperatures after normalising from 930 °C, can be attributed to the simultaneous variation in the size and volume fraction of vanadium carbides as described by the Zener model. However, for specimens hardened from 830 °C the Zener model predicts a decrease in prior austenite grain size, Fig. 10, with increasing normalising temperature although the reverse was observed.

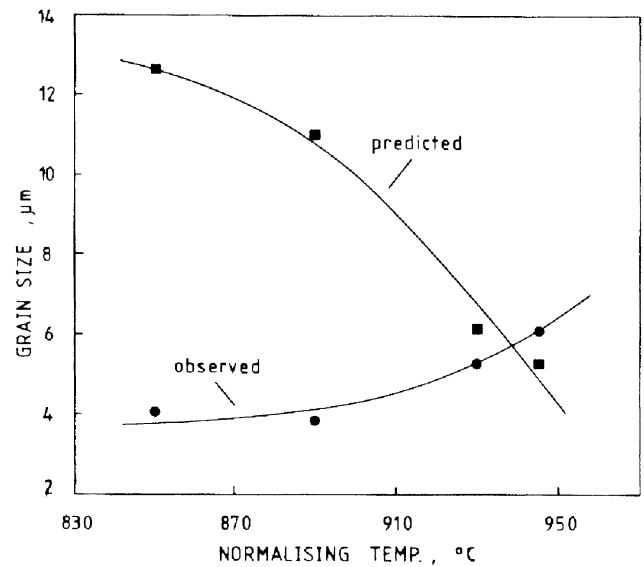


**Fig. 10** The variation in predicted and observed prior austenite grain size with normalising temperature in material hardened from 830 °C

A more realistic development [33] of the Zener model has determined the effect of spherical second phase particles on the pinning of grain boundaries of polygonal grains, which were assumed to be tetrakaidcahedra [34]. At the same time it was recognised that, even in the absence of pinning particles, a certain heterogeneity in grain size is necessary for grain growth. On the basis of this model, the critical radius of second phase particles,  $r_c$ , required to pin effectively grains of radius  $R$  was shown to be

$$r_c = (6Rf/\pi)(3/2 - 2/z)^{-1} \quad (4)$$

where  $f$  is the volume fraction of second phase particles and  $z$  is the grain size heterogeneity factor defined as the ratio of radii of growing grains and matrix grains. It can be seen that the critical particle size, above which grain growth can occur spontaneously, increases with increasing matrix grain size and volume fraction of precipitate and decreases with increasing heterogeneity of the matrix grain size [28]. The physical significance of  $z$  is that only large grains may grow in a polycrystalline structure.

The above model has given good agreement with experimental data for the growth of both austenite [28] and ferrite [31] grains in steels. The variation in critical particle diameter with normalising temperature and with hardening temperature after normalising from 930 °C is shown in Figs. 11 and 12, respectively. The value of the heterogeneity constant was usually about 1.75 but at high austenitising temperatures it increased

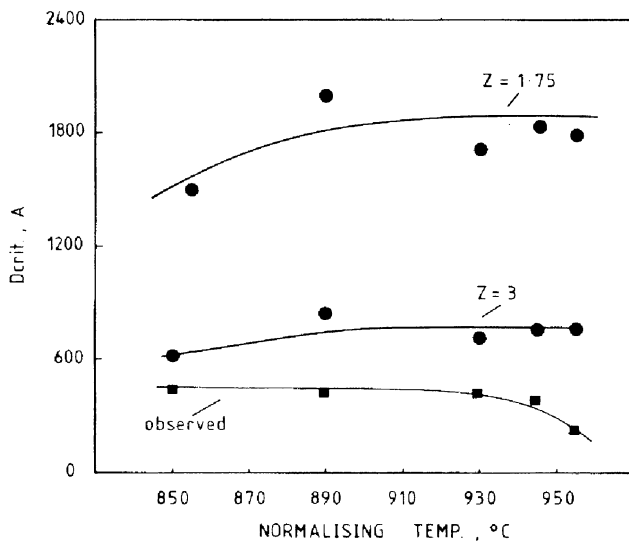


**Fig. 11** The variation in critical particle diameter,  $D_{crit}$ , with normalising temperature in as-normalised material

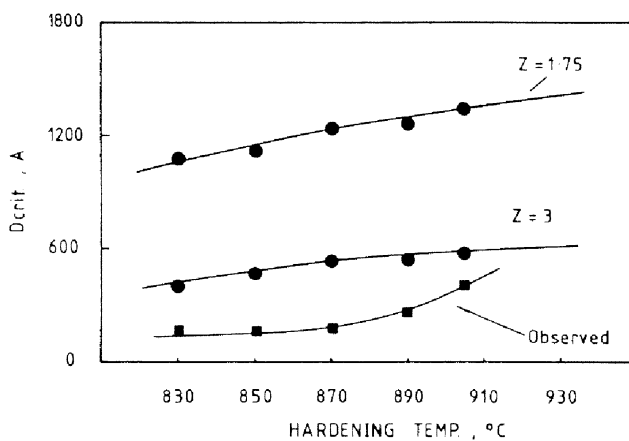


**Fig. 12** The variation in critical particle diameter,  $D_{crit}$ , with hardening temperature in material normalized from 930 °C

to  $\sim 3$ . As can be seen from Figs. 11 and 12 the measured sizes of vanadium carbide fall well below the calculated critical values, which indicates that the precipitates were very effective in retarding grain growth and may explain the fine grain sizes observed.

Although the results seem to agree well with the grain growth models, it was observed that very few carbides were actually present along the prior austenite grain boundaries. This is rather surprising in view of the grain growth inhibition models, which demand considerable grain boundary precipitation for effective growth inhibition. A similar observation is reported by Gladman and Pickering [28] and by Webster and Allen [21].

The latter workers suggested that the precipitate particles are not able to prevent grain boundary

movement completely. What probably happens is that a moving boundary is stopped only for a limited period of time. This period will increase with the number and size of the particles and decrease with increase in temperature [21]. The net result of a uniform dispersion of vanadium carbides is, therefore, to slow down the rate of grain boundary movement. As the vanadium carbides go into solution the rate of grain boundary movement increases rapidly and conditions become ideal for dominant growth by a few grains to occur.

The effect of a bimodal distribution of carbides on grain size

In the preceding discussion, the bimodal size distribution of vanadium carbides in the microstructure (primary and secondary), has not been taken into account. Gladman and Pickering [28] observed a similar bimodal size distribution of niobium carbides. They concluded that the carbides, which were effective in controlling austenite grain growth were only those which occurred as fine precipitates. Webster and Allen [21] on the other hand, suggested that the very fine vanadium carbides, which are precipitated during the second austenitising are too small to slow down grain boundary movement. They observed that only vanadium carbide particles larger than  $\sim 70$  nm were effective in inhibiting grain growth.

In the present work it was seen that grain growth in as-normalised specimens did not occur until all the primary vanadium carbides were dissolved, Fig. 5. On the other hand, it was observed that the grain size after the second austenitising, for the normalising temperatures of 930 and 910 °C, increased as the volume fraction of secondary vanadium carbides decreased, Fig. 3. The results of the present work, therefore, suggest that both types of vanadium carbides, those that remain undissolved after the initial austenitising (primary  $V_4C_3$ ) and those precipitated during re-austenitising (secondary  $V_4C_3$ ), are capable of inhibiting grain growth.

From the above considerations the question as to which type of vanadium carbide is more effective in inhibiting grain growth immediately follows. From Fig. 7 it is seen that the grain size after re-austenitising at 830 °C increases as the initial austenitising temperature is increased. This observation indicates that the presence of a large number of primary carbides and a few secondary carbides (low normalising temperature), results in a finer grain size than a small number of primary carbides and a large number of secondary carbides (high normalising temperature). This might

suggest that primary vanadium carbides are more effective in inhibiting grain growth than secondary carbides. However, an alternative explanation for the observed increase in grain size with increasing normalising temperature and a constant hardening temperature is possible, namely that of the “transmission” of the original austenite grain size.

Grain refinement by multi-cycle austenitising has been demonstrated by a number of investigators [35–38] and is now common practice in the manufacture of large rotor forgings. The heating rate employed for austenitising, however, is a very important parameter in controlling the degree of grain refinement achieved. Porter and Dabkowski [35], working with a 5Ni–Cr–Mo–V steel, investigated various heating rates and found that the grain refinement was much more pronounced at the faster heating rates employed. Homma [39] working with a 3.5Ni–Cr–Mo–V steel, found that re-austenitising at a heating rate of 50 °C/h resulted in no refinement of the grain size, whereas at a heating rate of 400 °C/h a refinement of approximately two ASTM numbers was obtained, irrespective of the original austenite grain size.

A mechanism that explains the effect of heating rate on the degree of grain refinement was proposed by Webster and Allen [21] as follows. When a martensitic structure is heated, carbides are precipitated at the boundaries of the martensite laths. As the temperature is increased the martensite laths become acicular ferrite grains whose further growth is prevented by the carbides at their boundaries. These carbides remain during the transformation to austenite, and just above the  $A_{c1}$  the newly formed austenite can grow until it meets the previous ferrite grain boundaries where its growth is stopped by the precipitated carbides. This results in a series of related acicular subgrains in the austenite. This is a very unstable structure due to the high grain boundary area, and as the temperature is increased, the subgrain boundaries acquire enough energy to grow past the restraining carbides. Once a subgrain has acquired enough energy to do this, it grows rapidly, sweeping the other subgrain boundaries before it until it occupies the whole austenite grain in which it occurs. This results in the previous austenite grain size being exactly reformed. With steels containing large amounts of carbide forming elements, the subgrain structure is stabilised, and a previous grain size can be transmitted to the austenite even at fast heating rates.

With very rapid heating the carbides precipitated at the austenite subgrain boundaries are much smaller than in slowly heated samples and hence the subgrain structure is less stable. Therefore when a sample is

rapidly heated to a temperature in the austenitising region the subgrains grow so rapidly that no subgrain has the chance to become dominant and the austenite grain size is not transmitted. Webster and Allen [21] showed that a very high heating rate of 1500 °C/h is required for the austenite grain size to be totally non-transmitted. The heating rate employed in the present work, 1500 °C/h, although fast enough for some grain refinement to be obtained, is believed to result in partial transmission of the austenite grain size developed during the initial austenitising. These considerations offer a second explanation for the observed increase in austenite grain size with increasing normalising temperature and a constant hardening temperature, Fig. 7.

## Conclusions

1. The prior austenite grain size increased with increasing austenitising temperature for both normalized and un-normalised material in accordance with a development of the Zener model.
2. A bimodal size distribution of vanadium carbides was observed, those that remain undissolved after the initial austenitising (primary  $V_4C_3$ ) and those precipitated during re-austenitising (secondary  $V_4C_3$ ).
3. The carbide size and spacing decreased with increasing austenitising temperature.
4. Both types of vanadium carbides, primary (coarse) and secondary (fine), are capable of inhibiting grain growth.
5. The critical particle size, above which grain growth can occur spontaneously, increases with increasing matrix grain size and volume fraction of precipitate and decreases with increasing heterogeneity of the matrix grain size.

**Acknowledgements** The present research is sponsored by the Hellenic Ministry of National Education and Religious Affairs and the European Union within the framework of the Operational Programme for Education and Initial Vocational Training (O.P. “Education”) -the latter being cofinanced by the European Social Fund, the European Regional Development Fund and national resources

## References

1. Gladman T (1997) The physical metallurgy of microalloyed steels. The Institute of Materials, London, p 235
2. Rodrigues JA, Dermonde JR (1985) *Mat Sci Tech* 1:29
3. Tamura I, Ouchi C, Tanaka T, Sekine H (1988) Thermo-mechanical processing of HSLA steels. Butterworths, Stoneham, MA, p 346

4. Wilcox JR, Honeycombe RWK (1987) *Mat Sci Tech* 3:849
5. Tither G, Shauhan Z (1992) *JOM, The Minerals, Metals and Materials Society* 44:115
6. Chen Z, Loretto MH, Cochrane RC (1987) *Mat Sci Tech* 3:836
7. Davis CL, Strangwood M (2002) *J Mat Sci* 37:1083
8. Mintz B, Wilcox JR, Crowther DN (1986) *Mat Sci Tech* 2:589
9. Lee CS, Lee KA, Li DM, Yoo SJ, Nam WJ (1998) *Mater Sci Eng A* 241:30
10. Nam WJ, Lee CS, Ban DY (2000) *Mater Sci Eng A* 289:8
11. Mattlock DK, Krauss G, Speer JG (2005) *Mat Sci Forum* 500:87
12. Gladman T, Pickering FB (1967) *J Ir St Inst* 205:653
13. Lui MW, LeMay I (1971) *Metallography* 4:443
14. Krahe PR, Desnoes M (1971) *Metallography* 4:171
15. Barraclough DR (1973) *Metallography* 6:465
16. Ashby MF, Ebeling R (1966) *Trans Met Soc AIME* 236:1397
17. Maropoulos S, Ridley N, Karagiannis S (2004) *Mater Sci Eng A* 380:79
18. Woodhead JH (1979) *Vanadium in high strength steel*. Vanitec, Chicago, p 78
19. Ridley N, Maropoulos S, Paul JDH (1994) *Mater Sci Tech* 10:239
20. Ballinger NK, Honeycombe RWK (1980) *Met Sci* 14:121
21. Webster D, Allen GB (1962) *J Ir St Inst* 200:520
22. Gladman T, Dulieu D (1974) *Met Sci* 8:167
23. Batte AD, Honeycombe RWK (1973) *J Ir St Inst* 211:284
24. Lapointe AJ, Baker TN (1982) *Met Sci* 16:207
25. Reed-Hill RE (1973) *Physical metallurgy principles*. D. Van Nostrand, New York, p 180
26. Harker D, Parker EA (1945) *Trans Am Soc Met* 34:156
27. Hillert M (1965) *Acta Met* 13:227
28. Gladman T, Pickering FB (1967) *J Ir St Inst* 205:653
29. Erasmus LA (1964) *J Ir St Inst* 202:128
30. Zener C (1949) *J Appl Phys* 20:950
31. Hobbs RM, Lorimer GW, Ridley N (1972) *J Ir St Inst* 210:757
32. Abrahamson EP (1970) In: Burke JJ, Weiss V (eds) *Ultrafine grain metals*. Syracuse Univ. Press, Syracuse, p 71
33. Pickering FB (1978) *Physical metallurgy and the design of steels*. Applied Sci. Publ., Essex, p 235
34. Gladman T (1966) *Proc Royal Soc* 294:298
35. Porter LF, Dabkowski DS (1970) In: Burke JJ, Weiss V (eds) *Ultrafine grain metals*. Syracuse Univ. Press, Syracuse, p 133
36. Grange RA (1971) *Met Trans* 2A:65
37. Palmiere EJ, Garcia CI, DeArdo AJ (1994) *Metall Trans* 25A:277
38. Flores O, Martinez L (1997) *J Mat Sci* 32:5985
39. Homma R (1974) *Trans J Ir St Inst Jap* 14:434